Pure Appl. Chem., Vol. 81, No. 3, pp. 417–432, 2009.
doi:10.1351/PAC-CON-08-08-03

Reliability and prediction of long-term performance of polymer-based materials*

Witold Brostow‡

Laboratory of Advanced Polymers and Optimized Materials (LAPOM), Department of Materials Science and Engineering, University of North Texas, 1150 Union Circle #305310, Denton, TX 76203-5017, USA

Abstract: The prediction of long-term performance from short-term tests is the bottom line of polymer science and engineering for users of polymer-based materials (PBMs)—which means for scientists, engineers, and laymen, or, literally, for everybody. Methods of prediction of mechanical properties (creep, stress relaxation, dynamic mechanical behavior, tension, etc.) based on the chain relaxation capability (CRC), the stress–time and temperature–time correspondence principles are presented. The methods can be applied even to small amounts of experimental data (2 or 3 isotherms or 2 or 3 stress levels) and can produce much better results than the still used 1955 Williams–Landel–Ferry (WLF) equation. Successful applications of the CRC approach include multiphase systems, including polymer liquid crystal (PLC) copolymers. An extension to the tribological properties of PBMs (in particular, scratch healing) is outlined. A quantitative definition of materials brittleness was formulated in 2006; it is connected to results in both the mechanics and tribology of PBMs.

Keywords: reliability; brittleness; tribology; long-term prediction; crack propagation.

SCOPE

Petroleum engineers prepare monomers from petroleum [1]. Then synthetic chemists create new polymers. Physical chemists (or else physicists or engineers) characterize the resulting materials. Rheologists melt the new materials and determine their properties in the molten state. Chemical engineers prescribe processing conditions. Others make injection molding machines or extruders. There are still more related specialties. They all have one property in common: the respective activities are of interest to other scientists and engineers rather than to society as a whole.

Historians tell us that the development of humanity can be divided into periods according to the function of the *materials* prevalently used; thus, the Stone Age, Bronze Age, Iron Age. Some historians tell us that we now live in the Plastics Age. Polymeric materials—popularly called plastics (sometimes rubbers)—are ubiquitous. We get polyethylene (PE) transparent bags for food bought in a market. There is plastic housing for cell phones and for computers. Small girls play with plastic dolls. In 2007, Boeing unveiled a new passenger plane called 787 or a Dreamliner; its frame is made from polymer-based materials (PBMs), in contrast to earlier planes with aluminum frames. What is important for the *users* of PBMs? Not synthesis, not rheological properties, not processing techniques. The only thing that counts for everybody is performance in service.

---

*Paper based on a presentation at POLYCHAR 16: World Forum on Advanced Materials, 17–21 February 2008, Lucknow, India. Other presentations are published in this issue, pp. 389–570.
‡E-mail: wbrostow@yahoo.com; <http://www.unt.edu/LAPOM/>

Laboratory tests take minutes or hours. Yet we need to predict the performance for years. Properties of metals do not change with time. PBMs are viscoelastic, therefore, their properties depend on time. Prediction of reliability and of long-term performance of PBMs is the subject of this article. In making such predictions, we have to rely on short-term tests. In the following paper, we shall discuss how this can be done.

BASIC CONCEPTS

The key question that comes out of the discussion above is simple: we have a PBM component in our hands and we would like to know: will it serve as long as we need it? Thus, the issue is that of *reliability*. How can our component stop serving too soon? There are two main dangers: either the component will be subjected to too large deformations or else it will be scratched and either significant wear or crack propagation will result. Thus, mechanics and tribology are involved. Tribology is pedantically defined as the science of interactions of moving surfaces [2]. In this review, we shall deal largely with mechanics and then in the final sections with tribology.

Thus, we first consider mechanical deformation. Energy is supplied to the polymeric component from the outside. The arrival of that energy can be fast, as in an impact event, or else slow, as in a controlled speed elongation. We know from tensile testing (or from compressive testing or 4-point bending, etc) that, up to a point, the material will resist the forces acting from the outside [3–6]. This brings us to the concept of the *chain relaxation capability* (CRC) [7]. *CRC is the amount of external energy dissipated by relaxational processes in a unit of time per unit weight of the viscoelastic material*. We realize that CRC pertains to a specific process of arrival of energy from the outside, such as in Charpy impact testing.

How does a viscoelastic material dissipate the energy? At least five options exist, as discussed earlier in Chapter 5 of [6]:

- transmission of energy along a given chain, manifesting itself as intensified vibrations of the segments
- transmission of energy from a given chain to its neighbors, mainly by entanglements but also by simple "touching" motions
- conformational rearrangements executed by the chains, such as from *cis* to *trans* conformation in carbonic chains
- elastic energy storage resulting from bond stretching and angle changes
- phase transformation toughening, discovered by Kim and Robertson in poly(butylene terephthalate) (PBT) [8] and seen later in conversion from hexagonal to monoclinic structure in isotactic polypropylene (PP) reported by Karger-Kocsis [9]

The penultimate item in the list above is also interesting. Textbooks of organic chemistry provide numbers for lengths of C–C bonds, also for the respective double and triple bonds. They also provide angles between such bonds. These numbers are true if *no external force* is applied. Earlier attempts to solve the problem we are now dealing with were unsuccessful among others because of neglecting changes in bond lengths and bond angles caused by the deformation.

What decides how large the CRC is? The primary factor is free volume v^f. It is defined as

$$v^f = v - v^* \tag{1}$$

All quantities in eq. 1 are usually expressed in $cm^3 \cdot g^{-1}$; v is the specific volume; v^* is called the incompressible or hard-core volume [10]; it is the remaining volume after all the free volume is "squeezed out" by going down to 0 K and applying a very high pressure. The more v^f there is, the higher the CRC.

In the following section, we shall see how the concept of CRC is applied to make predictions of several kinds on reliability and service performance.

TIME–TEMPERATURE SUPERPOSITION (TTS) PRINCIPLE

We have argued above that the free volume is very important, let us begin explaining why. Consider a nondestructive (i.e., relaxational) process at room temperature. Some such processes are quite slow, just as slow destructive processes exist (we shall talk about slow crack propagation below). Consider as an example a process that will take many years, such as creep caused by the gravitational field of the Earth only. However, if we raise the temperature by, say, 100 K, that is, from 20 to 120 °C, the same process will occur much faster. This leads us to the TTS principle, also called time–temperature equivalence principle: changes which will occur at a temperature of interest (which can be the room temperature, but can also be a different one) at long times can be observed and measured at elevated temperatures at shorter times.

Let us now consider an example of application of the TTS principle. We have investigated a number of PBMs, including a polymer liquid crystal (PLC) [11], namely, PET/0.6PHB, where PET = poly(ethylene terephthalate), PHB = *p*-hydroxybenzoic acid, and 0.6 is the mole fraction of the latter in the copolymer. One reason for inclusion of results for this particular material here are claims that the TTS principle applies only to so-called rheologically simple, that is, one-phase materials. PET/0.6PHB shows four coexisting phases, except at high temperatures such as 500 °C [12]. Thus, if these claims were valid, the TTS principle should not apply here.

We have determined tensile creep as well as tensile stress relaxation of PET/0.6PHB, each for a number of isotherms [13]. The creep results are presented as tensile compliance D in Fig. 1. That compliance is defined as

$$D(t) = \varepsilon(t)/\sigma = E^{-1}(t) \tag{2}$$

where t = time, ε = engineering strain, σ = engineering stress, and E = the tensile modulus. Thus, a constant stress σ is applied, causing changes in the strain, the compliance, and the modulus.

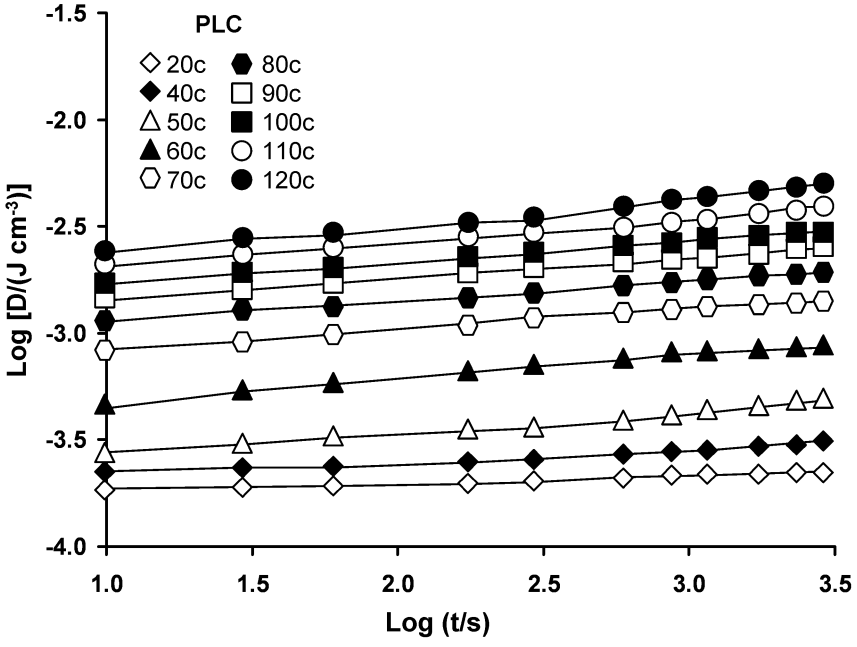

Fig. 1 Experimental tensile creep compliance of PET/0.6PHB PLC in logarithmic coordinates at 20 °C for temperatures indicated in the insert (after [13]).

Inspection of Fig. 1 tells us that at longer times the deformation is faster, hence, the compliance increases more rapidly. In other words, originally the material resists the external stress more but later its resistance becomes weaker. As expected, since at higher temperatures we have more free volume, there is less resistance and higher compliance.

We now proceed to accomplish the original task. We leave the curve for $T = 20$ °C as is; we shift all other curves to obtain a single continuous curve. The result is shown in Fig. 2. There is a large body of evidence [2–7] that the resulting so-called *master curve* provides us with prediction capabilities over 17 decades of time for 20 °C. Had we left a curve for a different temperature unmoved, we would have obtained a master curve for that particular temperature.

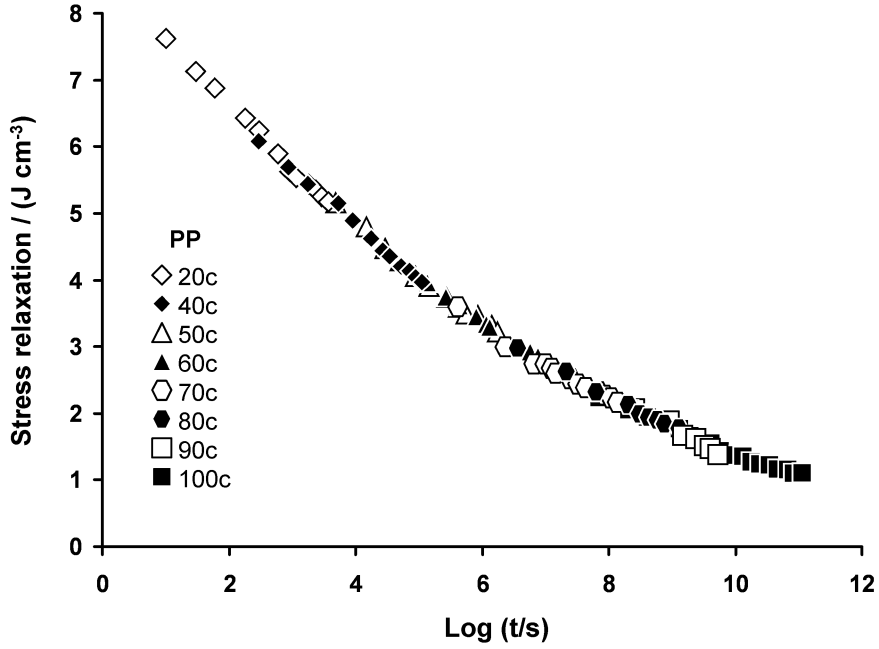

Fig. 2 Master curve of tensile creep compliance as a function of time for PET/0.6PHB PLC obtained using the results shown in Fig. 1; after [13].

The key question now is: How much should we move each of the individual isothermal curves?

That problem was solved many decades ago [3]. The relationship between the compliance and the modulus is defined in eq. 2; let us now work with the modulus since it seems to be used often. We define the *temperature shift factor*

$$a_T = \eta_\sigma T_{\text{ref}} \rho_{\text{ref}} / \eta_{\sigma\text{ref}} T \rho \tag{3}$$

where η_σ is the material viscosity corresponding to the applied stress σ, ρ is the mass density that is the reciprocal of specific volume: $\rho = v^{-1}$. The index ref pertains to the reference state, which in our case is 20 °C. In other words, we are applying the TTS principle:

$$E(T, t) = E(T_{\text{ref}}, t/a_T) \tag{4}$$

Equation 4 tells us that the modulus at a certain temperature T and time t is equal to the modulus at the reference temperature but at a different time, namely, t/a_T.

One can now sceptically say that we have not solved the problem how to apply the TTS principle, we have only reformulated it. Now the question is: how to calculate the temperature shift factor t/a_T? There have been several solutions of this problem, including an equation derived by the present author [4,7,6,14]:

$$\ln a_T = A_0 + A_1/(\tilde{v} - 1) \tag{5}$$

Here, A_0 and A_1 are constants for a given material; the latter is the Doolittle constant since it comes from his classical equation relating viscosity η (see eq. 3) to temperature via free volume [15]. Free volume as defined in eq. 1 is related to the reduced volume $\tilde{v}$

$$\tilde{v} = v/v^* \tag{6}$$

Actually, there are two more reduced quantities

$$\tilde{T} = T/T^* \text{ and } \tilde{P} = P/P^* \tag{7}$$

The hard-core temperature T^* is a measure of the strength of the intermolecular (in polymers intersegmental) interactions in a given material. The hard-core pressure P^* is a function of the interaction potential $u(R)$, and the binary radial distribution function $g(R)$ [16], where R is the interparticle distance.

To calculate $\tilde{v}$ or v^*, we need an equation of state. Good results have been obtained repetitively with the Hartmann–Haque equation [17]

$$\tilde{P}\,\tilde{v}^5 = \tilde{T}^{3/2} - \ln \tilde{v} \tag{8}$$

The term $\tilde{T}^{3/2}$ has a theoretical justification demonstrated by Litt [18]. Thus, one performs experimental determinations of the equation of state, that is, of $v(T, P)$. Several hundreds of such datapoints can be represented by eq. 8 with three unknowns, v^*, T^*, and P^* [19,20].

How good is eq. 5 in predicting the temperature shift factor? In Fig. 3, we show experimental values of a_T obtained by shifting, those calculated from eq. 5, and also those calculated from the Williams–Landel–Ferry (WLF) equation [3] developed in 1955. Within a certain temperature range, both equations provide good results; it is for this reason that the WLF equation is still in use. At lower temperatures, however, we see that the WLF equation provides really bad results. Actually, the WLF equation can be derived from our eq. 5 as a special case if one makes certain primitive and unfounded assumptions; see Chapter 10 in [4]. Here seems to lie "the evidence" that the TTS principle does not work. As we see in Figs. 1–3, the principle works beautifully for a very complex multiphase polymeric material. It is a particular implementation of the principle in the form of the WLF equation that at low temperatures provides outlandish results.

The next question we shall consider is: Are the values of a_T obtainable from eq. 5 valid only for creep experiments, or are they a material property? In creep experiments, we keep the stress level σ constant while we follow the evolution of the strain ε as a fuction of time; see again eq. 2. We can also invert the roles of stress and strain and perform *stress relaxation* experiments; that is, the strain level is quickly (but not quite instantly, within a short time t_0) brought to a constant value while we follow the evolution of stress with time; see Fig. 4.

We have performed stress relaxation experiments for the same PET/0.6PHB copolymer at several temperatures, created a master curve, and thus obtained experimental a_T values [13].

In Fig. 5, we show those values as a function of temperature along with those from creep experiments (the same as in Fig. 3) and with a_T results calculated from eq. 5. It is clear from Fig. 5 that within limits of the experimental accuracy all three sets of data coincide. Thus, $a_T(T)$ results are a true material property, independent of the experimental procedure used, and eq. 5 represents the temperature dependence of the shift factor accurately.

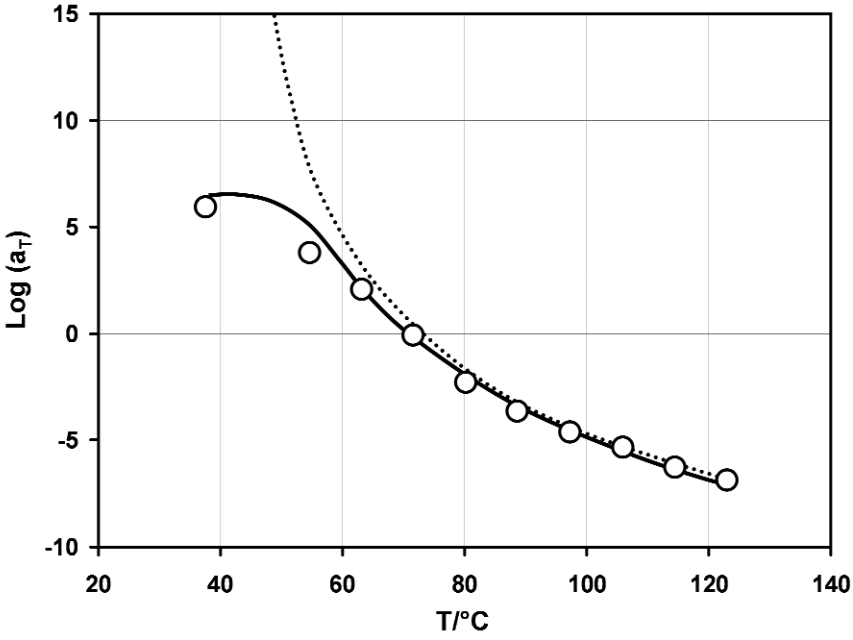

Fig. 3 The temperature shift factor a_T for PET/0.6PHB PLC obtained from the experimental creep data (circles, see Figs. 1 and 2); from the WLF equation (dotted line) and from eq. 5 (continuous line) in conjunction with eq. 8; after [13].

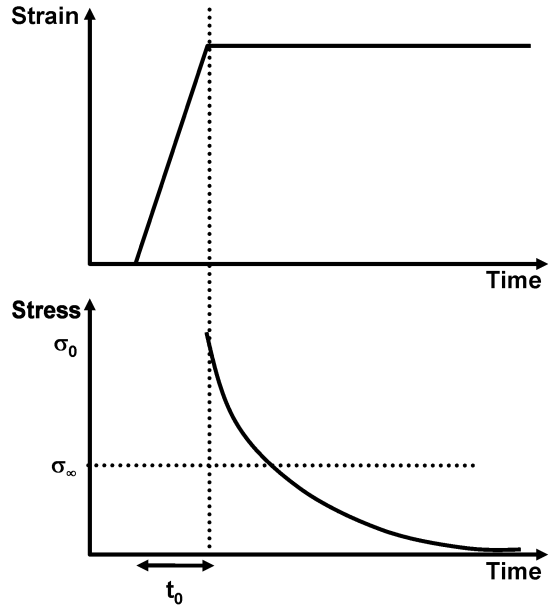

Fig. 4 Stress and strain evolution with time in the stress relaxation experiment.

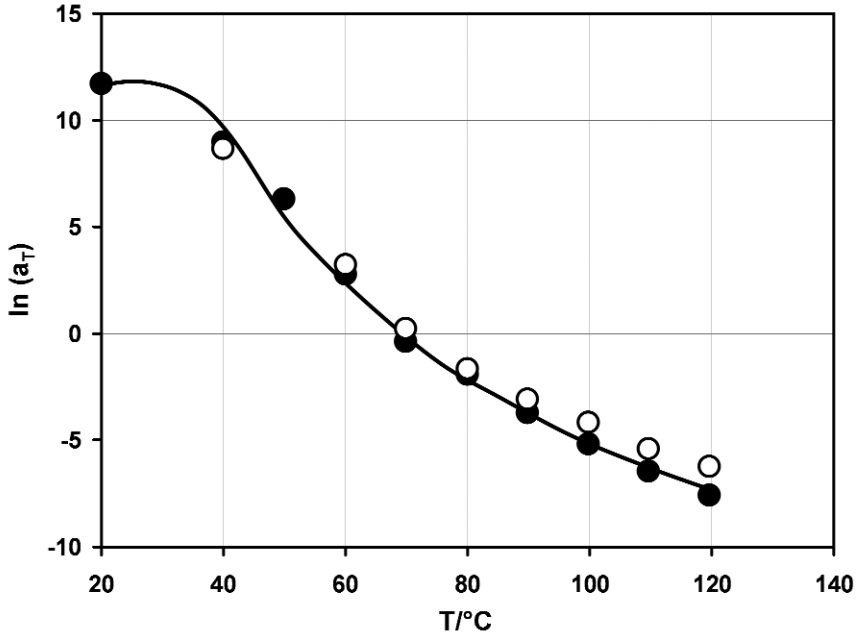

Fig. 5 The temperature shift factor a_T for PET/0.6PHB PLC: experimental creep data (filled circles); experimental stress relaxation data (open circles); calculated from eq. 5 (continuous line); after [13].

A still further question is: Do we need every time extensive experimental data to make predictions? In Fig. 1, we have seen results for 10 temperatures. Can we make reliable predicitions on the basis of two or three isotherms only?

Results of stress relaxation determinations for PET/0.6PHB PLC at a number of temperatures are displayed in Fig. 6. The respective master curve for 20 °C is shown in Fig. 7. Similarly, as in the case of creep, the master curve covers some 17 decades of time.

To respond to the question of minimizing the necessary input data, we show in Fig. 8 the temperature shift factor (this time log a_T, not ln a_T) calculated from data displayed in Figs. 6 and 7 plus experimental results for temperatures 130, 140, 150, and 160 °C. As always, there is a good agreement between experimental values (full circles) and those calculated from eq. 5 (the continuous line). Minor scatter of the points around the calculated line corresponds to experimental error. Parameters A_0 and A_1 have been obtained by solving an overdetermined system of eq. 5 in two unknowns. However, since there are two unknowns, it is possible to obtain the A_0 and A_1 parameters using experimental results for two isotherms only. This has been done using input from 20 and 160 °C. The results are also presented in Fig. 8: calculated values are represented by open circles and connected by a dotted line. We see that the lines are close to one another, as are filled and open circles. Thus, experimental determination of two isotherms only provides results close to those obtained from multiple isotherms, and thus sufficient for most prediction purposes.

We have focused above on a PLC because of the still lingering opinion that the TTS principle is applicable to one-phase PBMs only; we have proven the contrary. While it is not an intention of this review to list various applications of the principle in conjunction with eq. 5, let us provide one more example. Among others, good results have been obtained for creep of monofilament sutures of poly(vinylidene fluoride) (PVDF) [22].

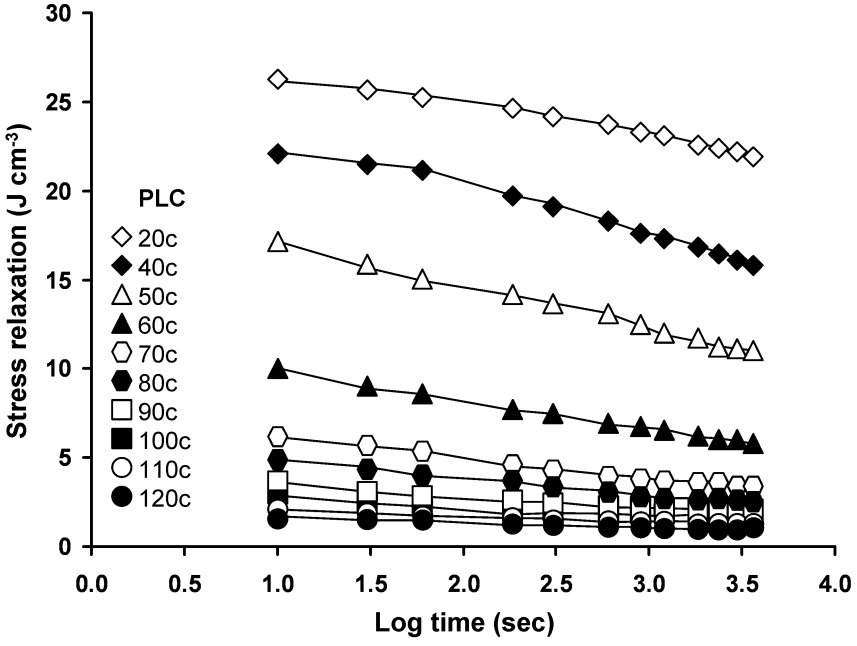

Fig. 6 Stress relaxation isotherms for PET/0.6PHB PLC; after [21].

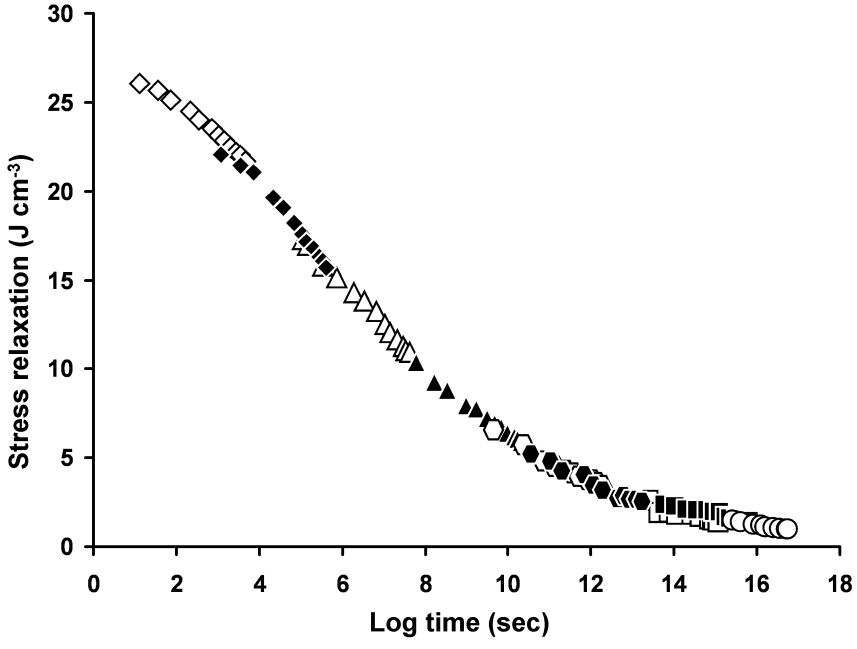

Fig. 7 Stress relaxation master curve for PET/0.6PHB PLC at 20 °C; after [21].

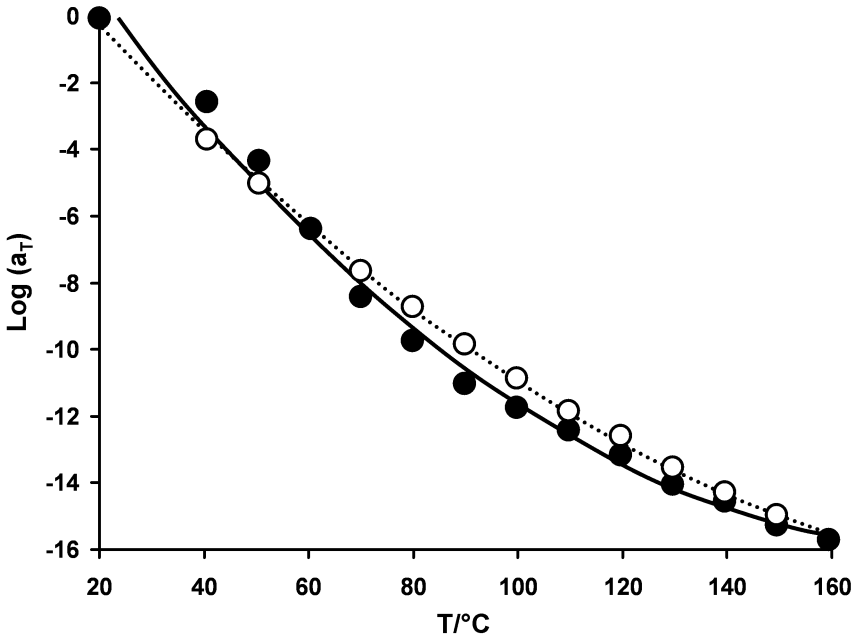

Fig. 8 The temperature shift factor obtained from results in Figs. 6 and 7; experimental results: filled circles: calculations from eqs. 5 and 8 using all data: continuous line; calculations from eq. 5 using data for two temperatures only: open circles and dotted line.

TIME–STRESS SUPERPOSITION (TSS) PRINCIPLE

In 1948, O'Shaughnessy showed that one can get a master curve for several decades of time performing experiments not isothermally at several temperatures but at several stress levels [23]. This was the first demonstration of the TSS or equivalence principle. Decades later, O'Shaughnessy's ideas were picked up by Maksimov and his colleagues at the Institute of Polymer Mechanics in Riga; the results have been described by Goldman [5]. Still, the shifting of curves has been done "manually". Only in 2000 an equation for the stress shift factor a_σ has been derived [24], starting once again from the Doolittle equation relating viscosity and free volume [15] and using the CRC concept. The result is

$$\ln a_\sigma = \ln [v(\sigma)/v_{\text{ref}}] + A_1/(\tilde{v} - 1) - 1/(\tilde{v}_{\text{ref}} - 1) + A_2/(\sigma - \sigma_{\text{ref}}) \tag{9}$$

where A_1 is the same Doolittle constant as before, A_2 is a new constant pertaining to effects of varying stress, while the index ref now pertains to the stress level of interest.

Actually, a more general equation has been derived in [24] for the variations of temperature T and stress σ

$$a_{T,\sigma} = (T_{\text{ref}}/T)\cdot[(v(T,\sigma)/v_{\text{ref}}(T_{\text{ref}},\sigma_{\text{ref}})]\cdot[\eta(T,\sigma)/\eta_{\text{ref}}(T_{\text{ref}},\sigma_{\text{ref}})] \tag{10}$$

From eq. 10, one obtains the convenient form

$$\ln a_{T,\sigma} = A_{T,\sigma} + \ln T_{\text{ref}}/T + \ln [v(T,\sigma)/v_{\text{ref}}] + A_1/(\tilde{v} - 1) + A_2/(\sigma - \sigma_{\text{ref}}) \tag{11}$$

It can be easily verified that eq. 11 can be reduced to eq. 5 by assuming $\sigma = \sigma_{\text{ref}}$. Similarly, eq. 11 can be reduced to eq. 9 by assuming $T = \text{const} = T_{\text{ref}}$ and identifying $A_{T,\sigma} = -1/(\tilde{v}_{\text{ref}} - 1)$.

We shall now verify how the TTS principle represented quantitatively by eq. 9 does the job it should. We shall work again with the multiphase PLC PET/0.6PHB. In Fig. 9, we show tensile creep compliance results for nine stress levels at 20 °C. The resulting master curve is shown in Fig. 10. Again,

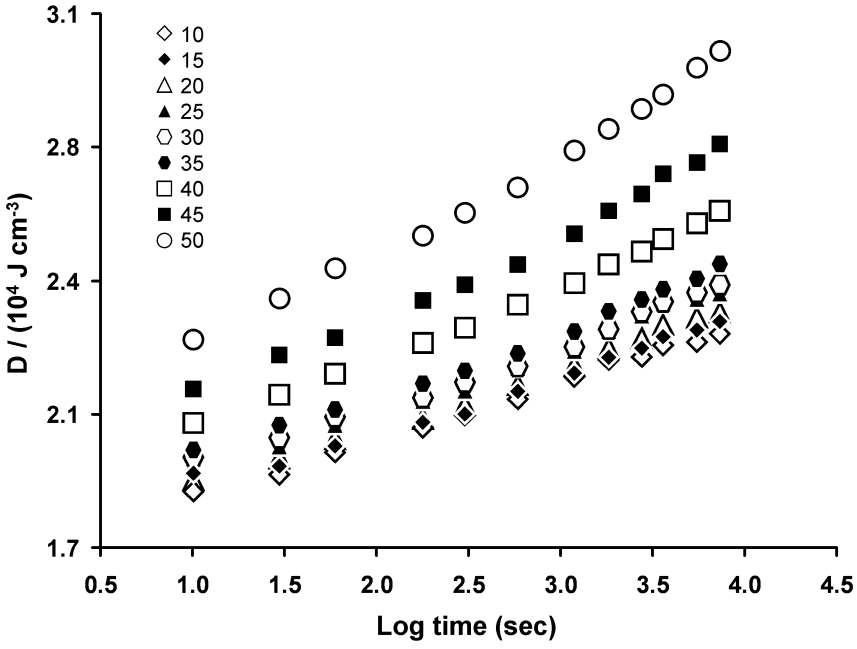

Fig. 9 Tensile creep compliance for PET/0.6PHB for nine stress levels at 20 °C; after [25].

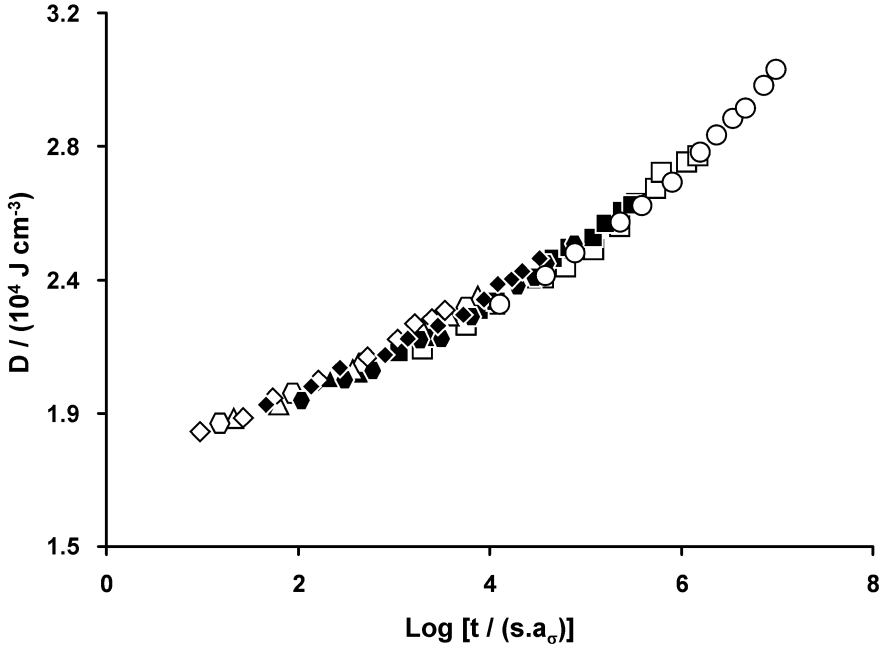

Fig. 10 Master curve of tensile creep compliance for PET/0.6PHB at 20 °C from the results in Fig. 9; after [25].

the superposition allows us to predict behavior at 20 °C for several decades beyond the actual experiments at that temperature.

We see that eq. 9 contains two parameters which need to be evaluated. Thus, in principle, one can use experimental results at two stress levels only to calculate the stress shift factor as a function of the stress applied. In Fig. 11, we present the results obtained on the basis of all stress level results as well as those obtained using only the extreme stress levels. When all data are used, we obtain from eq. 9 in conjunction with eq. 8: $A_1 = 5.10$ and $A_2 = -0.56$. When only the results for 10 and 50 J·cm^{-3} are used, we get $A_1 = 5.15$ and $A_2 = -0.54$. Thus, experiments at two stress levels only provide reliable results.

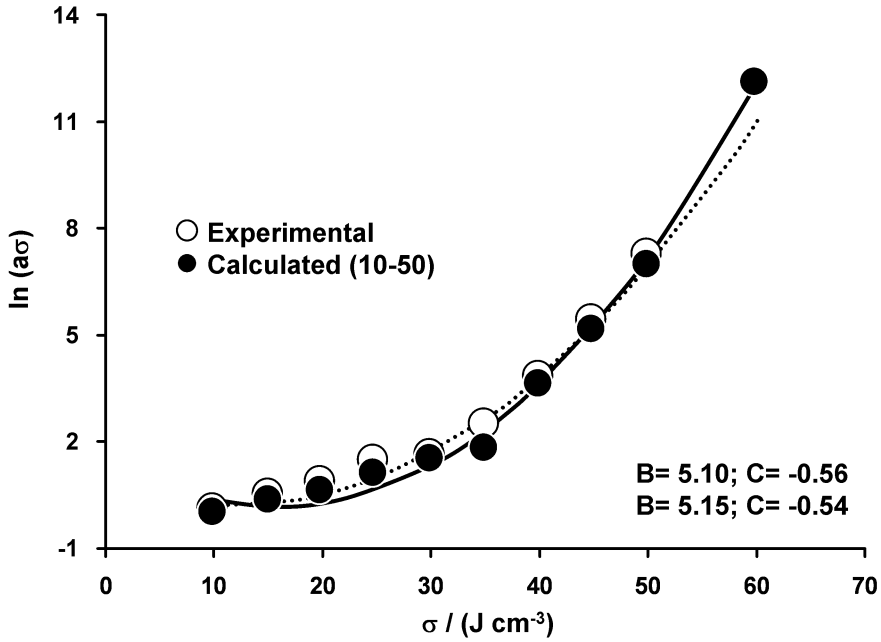

Fig. 11 The stress shift factor a_σ as a function of the stress level σ from results in Figs. 9 and 10 and using eqs. 5 and 8. The dotted line and the filled circles have been obtained using all nine sets of experimental data. The continuous line and the open circles have been obtained using data for two stress levels, 10 and 50 J·cm^{-3} only (1 J·cm^{-3} = 1 MPa).

SLOW CRACK PROPAGATION

In the beginning, we noted dangers to PBM performance resulting from deformation. The tacit assumption was that we are dealing with a material without micro- or macroscopic size defects. However, defects appear already in handling and in transport, even before arrival at the location where a given component will be used. One of the ways of quantifying the potential for crack propagation and fracture under a stress σ is in terms of the stress intensity factor

$$K_I = \alpha^* \pi^{1/2} \sigma h^{1/2} \tag{12}$$

Here, α^* is a geometric factor while h is the length of the existing crack.

There is experimental evidence that the stress intensity factor is a function of the crack propagation rate dh/dt, where as before t is time. A relation between the two quantities has been derived [26], namely,

$$\log K_I = (1/2)\cdot\log(\alpha^{*2} 2\Gamma E) + (1/2)\cdot\log[1 + (1/(\beta h_{cr})\cdot \mathrm{d}h/\mathrm{d}t] \tag{13}$$

Above, Γ is the surface energy per unit area. E is the elastic modulus, tensile if the stress σ is tensile, compressive if σ is compressive, etc. β is a time-independent proportionality factor characteristic for a material since it depends on CRC; the higher CRC, the lower β is. h_{cr} is defined by the fact that the crack will *not* propagate in a given material unless $h > h_{cr}$.

We shall now test the validity of eq. 13. Hoechst AG in Frankfurt/Main produces a variety of PEs. Their PEs have various molecular weights and various densities. Uniaxial tension was applied to various Hoechst PE specimens at several stress levels and with several initial crack lengths h_0. Results for three molecular weights are presented in Fig. 12. Each curve has been calculated from eq. 13. Points around each curve pertain to a single molecular weight M; different symbols pertain to different stress σ levels and to different values of h_0. Actually, both σ and h_0 have been taken into account in deriving eq. 13, but as we see, they do not appear in the final equation. In agreement with predictions of eq. 13, points for a PE with a given molecular weight form a single curve, independently of σ and h_0.

To see the significance of Fig. 12 better, return to the contributions to CRC listed in the second section. Longer chains absorb more energy by relaxation, internally as well as by transmission of energy to neighboring chains. With more energy absorption, the crack propagation rate dh/dt should be lower. This is indeed what Fig. 12 shows; the molecular weight decreases in the order $M_C > M_B > M_A$.

We have discussed above the fact that CRC increases when free volume v^f increases. Since the mass density $\rho = 1/v$, lower density is associated with higher free volume (see again eq. 1). In Fig. 13, we display four curves similar as in Fig. 12 but now for different PE densities. Figure 13 represents a direct confirmation of the CRC concept. The lower the density, that is, the higher the free volume, the lower is the crack propagation rate dh/dt.

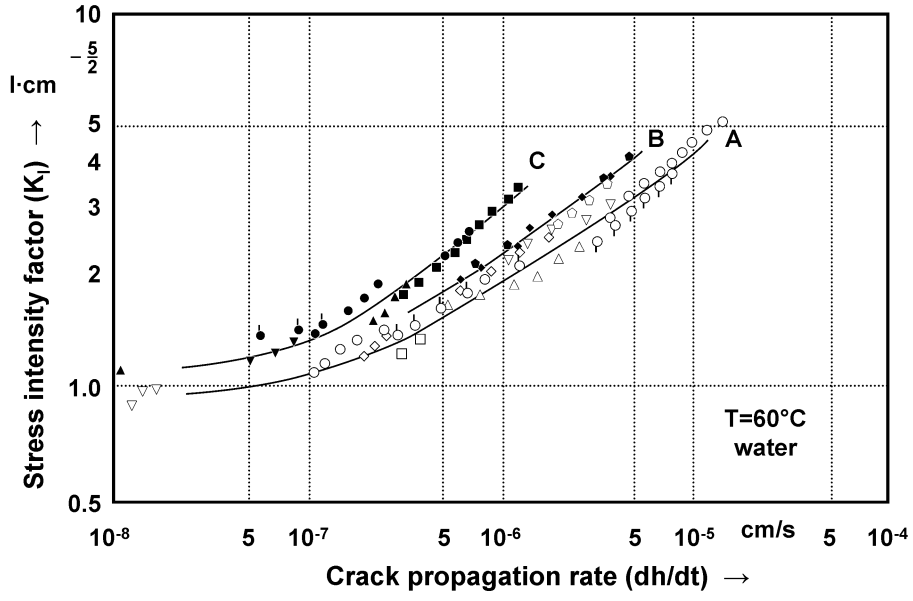

Fig. 12 Stress intensity factor K_I as a function of the crack propagation rate dh/dt for a series of Hoechst PEs in water at 60 °C; after [26]. Each series has a different molecular weight.

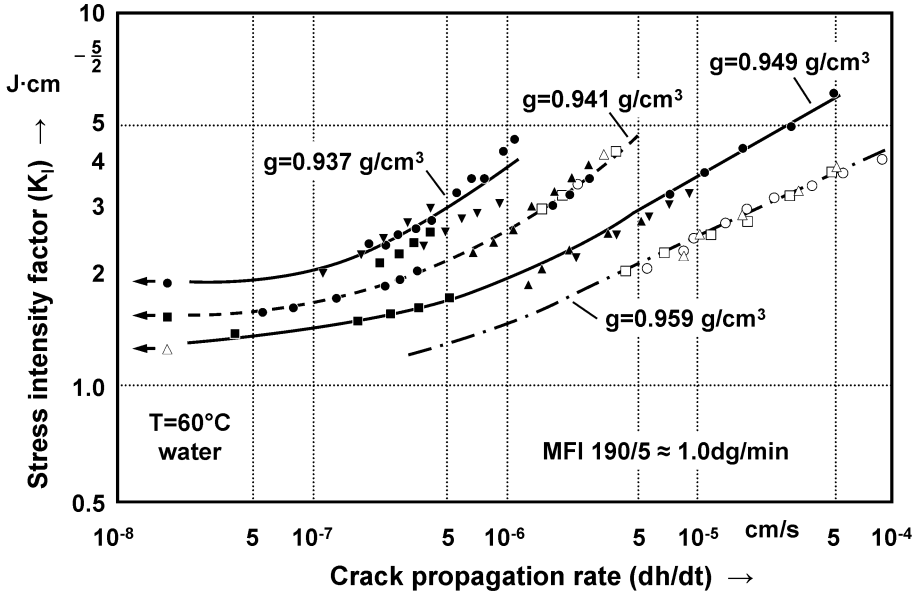

Fig. 13 Stress intensity factor K_I as a function of the crack propagation rate dh/dt for a series of Hoechst PEs in water at 60 °C; after [26]. Each series has a different density.

DUCTILE–BRITTLE IMPACT TRANSITION TEMPERATURE

Materials at low temperatures fail in a brittle way, at high temperatures in a ductile way. There exists the ductile–brittle impact transition temperature T_I which is a function of the stress concentration factor K_t. At that temperature, half of the specimens fail in a brittle way while the other half fail in a ductile way, something the practitioners of scanning electron microscopy (SEM) apparently are able to evaluate visually. The stress concentration factor has a similar name as the stress intensity factor discussed above but the definition is

$$K_t = 1 + 2(h/l)^{1/2} \tag{14}$$

Here, h is the crack length as before while l is the radius of curvature at the tip of the crack.

Equation 14 tells us that longer cracks are more dangerous while cracks with a large radius at the tip are less dangerous. The physical significance of K_t is: how many times is the stress at the tip of the crack larger than the nominal stress σ applied to the entire material.

Following the CRC concept, we assume that the transition temperature T_I is related to free volume. There is more v^f at elevated temperatures, and it is for this reason that above T_I we have ductile behavior and below that temperature brittle behavior. The derivation of a relationship between K_t and T_I is provided in Chapter 10 of [4]. Our eq. 5 for the temperature shift factor is used in the derivation. The final result is

$$K_t = F \cdot \exp[-A_1/(\tilde{v} - 1)] \tag{15}$$

Here, the material parameter F is related to the constant A_0 in eq. 5 and A_1 is the Doolittle constant as before. The transition temperature T_I is implicit since in the equation it is represented by the reduced volume at that temperature $\tilde{v}_1(T_1)$.

Validity of eq. 15 was tested for low-density PE (Chapter 10 of [4]). The results are presented in Fig. 14. We see that eq. 15 represents the experimental results within limits of the experimental accuracy. Thus, experimental determination of two $T_I(K_t)$ pairs and an equation of state $\tilde{v}(T)$ suffice to de-

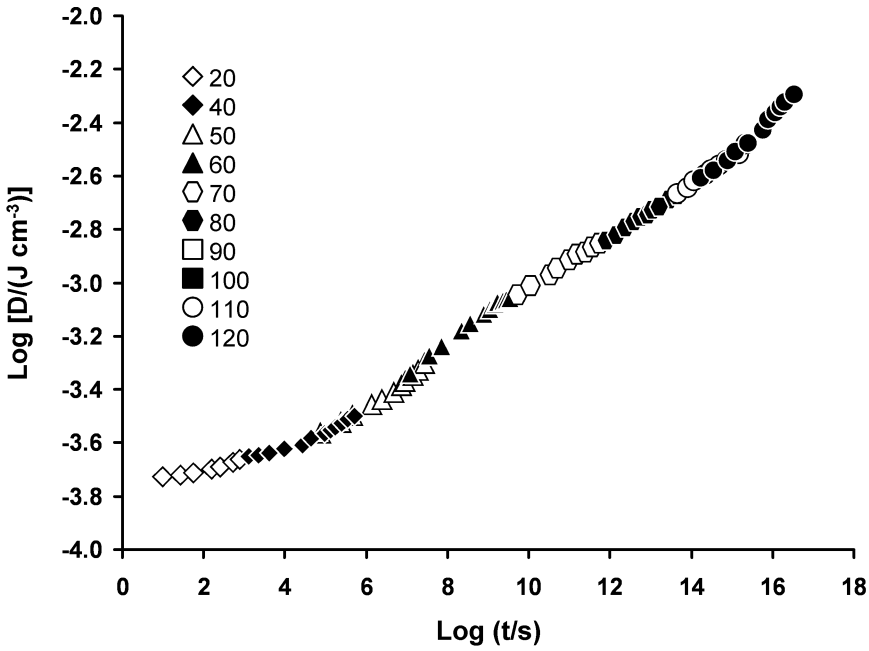

Fig. 14 Ductile–brittle impact transition temperature T_I as a function of the stress concentration factor K_t for low-density PE; after Chapter 10 of [4].

termine the parameters F and A_1 and thus predict the whole curve. We recall that the Doolittle parameter A_1 can be already known, determined by methods discussed above in the third section; then one $T_I(K_t)$ will suffice.

SCRATCH AND WEAR RESISTANCE

As noted in the beginning of the second section, crack propagation and failure can begin from a scratch on the material surface. Together with friction, abrasion, and wear determination, scratch resistance determination belongs to tribology. There are review articles on polymer tribology, on experiments [27,28] as well as on computer simulations [29].

A good method of determination of scratch resistance relies on a microscratch tester [27,30,31]. One determines the instantaneous or *penetration depth* R_p created by an indenter. Viscoelasticity of PBMs is here an advantage; inside the groove, the bottom goes up because of the rapid healing process; the healing or *residual depth* R_h is measured 2 min after the passage of the indenter. The viscoelastic recovery is defined [30] as

$$f = 100\ \%(R_p - R_h)/R_h \tag{16}$$

The extent of the recovery can be quite high, such as 70 or even 80 %.

The same microscratch tester provides also the capability of *sliding wear* determination, which consists in multiple scratching along the same groove [29,31,32]. Performing such experiments, we have found for three polymers that after 10 or so runs the depth of the groove does not change anymore [32]. This *strain hardening in sliding wear* has been subsequently found also for a number of other polymers.

BRITTLENESS OF MATERIALS

It would be nice if one could assume that strain hardening in sliding wear takes place in every polymer. Then, for a given force applied via the indenter we would know the final depth of the groove. However, we have found one exception: polystyrene (PS) does not exhibit this phenomenon. With subsequent runs of the indenter, the depth of the groove keeps on increasing. We have investigated this exception thoroughly [33–35].

The natural question is: Why is the behavior of PS exceptional? A popular answer is: Because PS is brittle. However, we remember from the sixth section that the brittleness—or lack of thereof—are evaluated by visual inspection of SEM results. In this situation, we have decided that a quantitative definition of brittleness is needed. We have provided such a definition in 2006 [31]

$$B = 1/(\varepsilon_b E') \tag{17}$$

Here, ε_b is the strain at break in tensile testing while E' is the storage modulus determined by dynamic mechanical analysis (DMA) at the frequency of 1.0 Hz at the temperature of interest. The DMA technique is well explained by Lucas and her colleagues [36] and also by Menard [37]. Briefly, E' represents the solid-like or elastic component of viscoelasticity. The definition (eq. 17) corresponds also to the existing before everyday use of the term brittleness [38,39].

We do not display here specific results on brittleness since some are reported in [31] and more were presented at POLYCHAR 15 [40]. It is important that a connection between the viscoelastic recovery f (eq. 16) in sliding wear and the brittleness has been established. For room temperature, we have

$$B = b_1 e^{-f/b_2} \tag{18}$$

where b_1 and b_2 are constants. Equation 18 applies to all polymers studied, with a large variety of chemical structures. This time, PS is no exception. It has the lowest found recovery f and by far the highest brittleness. We note that mechanics and tribology are considered to be two distinct disciplines. Equation 18 provides a connection between the two classes of properties. Roald Hoffmann, in an invited lecture at the POLYCHAR 13 World Forum on Advanced Materials, Singapore, 3–8 July 2005, as well as Rustum Roy [41] are pointing out that we need integration of science and engineering, rather than compartmentalization. Equation 18 is also an example that this can be done.

How do we use the concept of brittleness for the present purposes? If we have a material with high brittleness, then reliable performance is *not* expected. This is known also from everyday life: a PS coffee cup can be crushed easily.

ACKNOWLEDGMENTS

Some of the results presented here have been obtained with support of the Robert A. Welch Foundation, Houston (grant no. B-1203); Hoechst AG, Frankfurt/Main; and the Institute of Polymer Mechanics, University of Latvia, Riga.

REFERENCES

1. E. F. Lucas, C. R. E. Mansur, L. Spinelli, Y. G. C. Queirós. *Pure Appl. Chem.* **81**, 473 (2009).
2. E. Rabinowicz. *Friction and Wear of Materials*, 2nd ed., John Wiley, New York (1995).
3. J. D. Ferry. *Viscoelastic Properties of Polymers*, 3rd ed., John Wiley, New York (1980).
4. W. Brostow, R. D. Corneliussen (Eds.). *Failure of Plastics*, Hanser, Munich (1986, 1989, 1992).
5. A. Y. Goldman. *Prediction of Deformation Properties of Polymeric and Composite Materials*, American Chemical Society, Washington, DC (1994).
6. W. Brostow (Ed.). *Performance of Plastics*, Hanser, Munich (2000).

7. W. Brostow. *Makromol. Chem. Symp*. **41**, 119 (1991).
8. J. Kim, R. E. Robertson. *J. Mater. Sci*. **27**, 3000 (1992).
9. J. Karger-Kocsis. *Polym. Eng. Sci*. **36**, 203 (1996).
10. P. J. Flory. *Selected Works*, Vol. 3, Stanford University Press (1985).
11. W. Brostow (Ed.). *Polymer Liquid Crystals, Vol. 3: Thermophysical and Mechanical Properties*, Chapman & Hall, London (1998).
12. W. Brostow, M. Hess, B. L. López. *Macromolecules* **27**, 2262 (1994).
13. W. Brostow, N. A. D'Souza, J. Kubát, R. D. Maksimov. *J. Chem. Phys*. **110**, 9706 (1999).
14. W. Brostow. *Mater. Chem. Phys*. **12**, 557 (1985).
15. A. K. Doolittle. *J. Appl. Phys*. **22**, 1031 (1951).
16. W. Brostow, W. Szymanski. *J. Rheol.* **30**, 877 (1986).
17. B. Hartmann, M. A. Haque. *J. Appl. Phys*. **58**, 2831 (1985).
18. (a) M. H. Litt. *Trans. Soc. Rheol*. **20**, 47 (1976); (b) M. H. Litt. In *Molecular Basis of Transitions and Relaxations*, D. Meier (Ed.), p. 311, Gordon & Breach, New York (1978).
19. J. M. Berry, W. Brostow, M. Hess, E. G. Jacobs. *Polymer* **39**, 4081 (1998).
20. W. Brostow, V. M. Castaño, G. Martinez-Barrera, D. Pietkiewicz. *Physica B* **344**, 206 (2004).
21. A. E. Akinay, W. Brostow, V. M. Castaño, R. Maksimov, P. Olszynski. *Polymer* **43**, 3593 (2002).
22. J. F. Mano, J. L. Lopes, R. A. Silva, W. Brostow. *Polymer* **44**, 4293 (2003).
23. M. T. O'Shaughnessy. *Textile Res. J*. **18**, 263 (1948).
24. W. Brostow. *Mater. Res. Innovat*. **3**, 347 (2000).
25. A. E. Akinay, W. Brostow. *Polymer* **42**, 4527 (2001).
26. W. Brostow, M. Fleissner, W. F. Müller. *Polymer* **32**, 419 (1991).
27. W. Brostow, J.-L. Deborde, M. Jaklewicz, P. Olszynski. *J. Mater. Ed*. **25**, 119 (2003).
28. N. K. Myshkin, M. I. Petrokovets, A. V. Kovalev. *Tribol. Int.* **38**, 910 (2005).
29. W. Brostow, R. Simões. *J. Mater. Ed*. **27**, 19 (2005).
30. W. Brostow, B. Bujard, P. E. Cassidy, H. E. Hagg, P. E. Montemartini. *Mater. Res. Innovat*. **6**, 7 (2002).
31. W. Brostow, H. E. Hagg Lobland, M. Narkis. *J. Mater. Res*. **21**, 2422 (2006).
32. W. Brostow, G. Damarla, J. Howe, D. Pietkiewicz. *e-Polymers* no. 025 (2004).
33. M. D. Bermudez, W. Brostow, F. J. Carrion-Vilches, J. J. Cervantes, D. Pietkiewicz. *e-Polymers* no. 001 (2005).
34. M. D. Bermudez, W. Brostow, F. J. Carrion-Vilches, J. J. Cervantes, G. Damarla, J. M. Perez. *e-Polymers* no. 003 (2005).
35. M. D. Bermudez, W. Brostow, F. J. Carrion-Vilches, J. J. Cervantes, D. Pietkiewicz. *Polymer* **46**, 347 (2005).
36. E. F. Lucas, B. G. Soares, E. Monteiro. *Caracterização de polimeros*, e-papers, Rio de Janeiro (2001).
37. K. P. Menard. *Dynamic Mechanical Analysis: A Practical Introduction*, 2nd ed., CRC Press, Boca Raton, FL (2008).
38. E. Werwa. *J. Mater. Ed*. **22**, 18 (2000).
39. H. E. Hagg Lobland. *J. Mater. Ed*. **27**, 29 (2005).
40. W. Brostow, H. E. Hagg Lobland. *Polym. Eng. Sci*. **48**, 1982 (2008).
41. R. Roy. *IUMRS Facets* **4**, 18 (2005).